Ab Initio Approaches to Nuclear Reactions

Petr Navrátil

TRIUMF, 4004 Wesbrook Mall, Vancouver, BC V6T 2A3, Canada

Abstract

The exact treatment of nuclei starting from the constituent nucleons and the fundamental interactions among them has been a long-standing goal in nuclear physics. In addition to the complex nature of nuclear forces, one faces the quantum-mechanical many-nucleon problem governed by an interplay between bound and continuum states. In recent years, significant progress has been made in *ab initio* nuclear structure and reaction calculations based on input from QCD employing Hamiltonians constructed within chiral effective field theory. In this contribution, we first present a brief overview of recent achievements of various *ab initio* nuclear reaction approaches and then focus on the newly developed techniques, the no-core shell model with continuum (NCSMC) capable of describing simultaneously both bound and scattering states in light nuclei.

Keywords: *Ab initio calculations; low-energy nuclear reactions, resonances, halo nuclei*

1 Introduction

One of the central goals of nuclear physics is to come to a basic understanding of the structure and dynamics of nuclei, quantum many-body systems exhibiting bound states, unbound resonances, and scattering states, all of which can be strongly coupled. *Ab initio* (i.e., from first principles) approaches attempt to achieve such a goal for light nuclei. Over the past fifteen years, efficient techniques such as the Green's function Monte Carlo (GFMC) [1], *ab initio* NCSM [2], Coupled Cluster Method (CCM) [3–5] or nuclear lattice effective field theory (EFT) [6] have greatly advanced our understanding of bound-state properties of light nuclei starting from realistic nucleon-nucleon (NN) and three-nucleon ($3N$) interactions. On the other hand, a fully-developed fundamental theory able to address a large range of nuclear scattering and nuclear reaction properties is still missing, particularly for processes involving more than four nucleons overall. Better still, achieving a realistic *ab initio* description of light nuclei requires abandoning the "traditional" separated treatment of discrete states and scattering continuum in favor of a unified treatment of structural and reaction properties. The development of such a unified fundamental theory of light nuclei is key to refining our understanding of the underlying forces across the nuclear landscape: from the well-bound nuclei to the exotic nuclei at the boundaries of stability that have become the focus of the next generation experiments with rare-isotope beams, to the low-energy fusion reactions that represent the primary energy-generation mechanism in stars, and could potentially be used for future energy generation on earth.

In this contribution, we present a brief overview of the emerging field of *ab initio* calculations of nuclear reactions in Section 2. In Section 3, we describe the recently

introduced *ab initio* many-body approach to nuclear bound and continuum states, the no-core shell model with continuum (NCSMC) that combines the resonating-group method (RGM) [7] with the *ab initio* no-core shell model (NCSM) [8]. In Section 4, we discuss recent applications of the NCSMC to the description of ^{7}He resonances, we investigate the $3N$ interaction effects in the nucleon-^{4}He scattering, we highlight the introduction of the three-body clusters in the description of ^{6}He, and present preliminary study of the continuum effects in the low-lying resonances of ^{9}Be. Conclusions are given in Section 5.

2 *Ab initio* approaches to nuclear reactions

Because of their importance nuclear reactions attract much attention, and there have been many interesting new developments in the recent past. In this section we will give a brief and non-exhaustive overview of the theoretical efforts devoted to *ab initio* approaches to nuclear reactions, and in particular scattering of light nuclei.

By *ab initio* approaches we mean methods, in which all the nucleons involved in the process are treated as active degrees of freedom, and the antisymmetrization of the many-body wave functions is treated exactly. Further, the NN interactions among all participating nucleons are realistic, i. e., describe accurately NN scattering and the deuteron. Finally, the approximations used in the calculations should be controllable in a sense that it should be feasible to arrive at or to extrapolate to an exact result with a specified uncertainty. We note that, in general, the $3N$ force that provides a realistic description of the three-nucleon system should also be considered in *ab initio* calculations.

In the three- and four-nucleon sectors there has been remarkable progress over the past decade: the Faddeev [9], Faddeev–Yakubovsky (FY) [10, 11], Alt, Grassberger and Sandhas (AGS) [12, 13], hyperspherical harmonics (HH) [14], Lorentz integral transform (LIT) methods [15–17], RGM [18], etc., are among the best known of several numerically exact techniques able to describe reactions observables starting from realistic NN and in some cases also $3N$ forces.

Going beyond four nucleons there are fewer *ab initio* or *ab initio* inspired methods able to describe reactions observables starting from realistic forces. Only very recently the Green's function Monte Carlo (GFMC) [19], the no-core shell model combined with the resonating group method (NCSM/RGM) [20, 21] and the fermionic molecular dynamics [22] have made steps in this direction.

Among the recent developments in the $A = 4$ scattering and reaction calculations we highlight the new capability to include properly the Coulomb interaction in momentum space [12, 13] and to include the three-nucleon interaction in the p-^{3}H Faddeev–Yakubovsky configuration space calculations [11]. A benchmark for the n-^{3}H low-energy elastic cross section calculation has been performed by the FY, AGS and HH methods using different NN potentials [23]. The main conclusion of this work is the failure of the existing NN forces to reproduce the n-^{3}H total cross section. Remarkable recent results are the p-^{3}He scattering calculations performed using the hyperspherical harmonic basis, which demonstrated that the new NN plus $3N$ interactions derived within chiral effective field theory (EFT) reduce noticeably the discrepancy observed for the A_y observable [24]. Further, with the same Hamiltonian, the low-energy total n-^{3}H cross section calculated by the HH method was found in improved agreement with the data [25].

In a ground-breaking development, the AGS method has been generalized to calculations of the n-^{3}H scattering above the four-nucleon breakup threshold [26]. This allowed to calculate the elastic cross section of 14.1 MeV neutrons. This is in particular important as such high-energy neutrons are produced in the deuteron-triton fusion.

The first *ab initio* scattering calculation for a system with $A > 4$ was performed within the GFMC approach. The n-α low-lying $J^\pi = 3/2^-$ and $1/2^-$ P-wave resonances as well as the $1/2^+$ S-wave non-resonant scattering below 5 MeV center of mass (c.m.) energy were obtained using the AV18 NN potential with and without the three-nucleon force, chosen to be either the Urbana IX or the Illinois-2 model [19]. The results of these calculations revealed sensitivity to the inter-nucleon interaction, and in particular to the strength of the spin-orbit force. New developments of the GFMC applications to nuclear reactions include calculations of spectroscopic overlaps for light nuclei [27] and calculations of the asymptotic normalization constants (ANC) by integral relations with the variational Monte Carlo (VMC) wave functions [28].

The FMD approach has been applied quite successfully to the description of the radiative capture cross section (S-factor) of the ^{3}He(α,γ)^{7}Be reaction important for astrophysics. The FMD calculations describe new experimental data both at low energy (below 100 keV) as well as at high energy (from 1 MeV to 2.5 MeV) [29].

As an interesting theoretical development to the many-body scattering, we mention the approach based on the variational description of continuum states in terms of integral relations [30] that may be used to directly apply the bound-state many-body techniques to scattering. A variation of this approach has been explored in the $A = 5$ scattering in Ref. [31]. Further, the use of bound-state methods to calculate scattering properties with possible applications for lattice calculations has been investigated in Ref. [32].

There are also some recent attempts to describe the nuclear scattering in an effective field theory approach. In particular, the pionless EFT combined with the RGM was successfully applied to three- and four-nucleon bound state and scattering calculations [33].

In a big jump in mass number, we note that the ^{17}F low-lying states were recently investigated within the coupled-cluster (CC) approach with the Gamow–Hartree–Fock basis that incorporates effects of the continuum [34]. The calculation resulted in a good description of the $1/2^+$ proton halo state in ^{17}F. It was shown that the continuum effects are essential to obtain these results and that the proton halo state single-particle energy is not affected by short-range correlations in the nuclear interactions.

The CC theory has been recently combined with the LIT method to calculate the photodisintegration of ^{4}He and, in particular, the giant dipole resonance in ^{16}O [35].

Using the Gamow–Hartree–Fock basis, the CCM was used for the first time to calculate *ab initio* elastic proton scattering on a nucleus as heavy as ^{40}Ca [36]. Elastic scattering of a nucleon on a target nucleus can be computed from the one-nucleon overlap functions. These are calculated within the CC theory. The obtained cross sections at low-energy for elastic proton scattering on ^{40}Ca were found in a fair agreement with experiment.

As a completely new development, *ab initio* calculations of nuclear scattering and reactions on the lattice has been explored in Ref. [37]. Adiabatic projection method was implemented and tested in elastic fermion-dimer scattering in lattice effective field theory. Such calculation corresponds to neutron-deuteron scattering in the spin-quartet channel at leading order in pionless effective field theory. The method adapts features of the resonating group method [7] in a similar fashion as in the NCSM/RGM approach [38] discussed in the subsequent sections.

3   No-core shell model with continuum

In this section we briefly overview the newly introduced approach to nuclear bound and continuum states, the no-core shell model with continuum [39, 40]. This approach adopts an extended model space that, in addition to the continuous binary-cluster $(A-a, a)$ NCSM/RGM states, with $A-a$ and a nucleons in the heavier and

the lighter cluster, respectively, encompasses also square-integrable NCSM eigenstates of the complete A-nucleon system. Such eigenstates introduce in the trial wave function short- and medium-range A-nucleon correlations that in the binary-cluster NCSM/RGM formalism have to be treated by including a large number of excited states of the clusters.

3.1 NCSM

The *ab initio* NCSM is a nuclear-structure technique appropriate for the description of bound states or for approximations of narrow resonances. Nuclei are considered as systems of A non-relativistic point-like nucleons interacting through realistic inter-nucleon interactions. Translational invariance as well as angular momentum and parity of the system under consideration are conserved. The many-body wave function is cast into an expansion over a complete set of antisymmetric A-nucleon harmonic oscillator (HO) basis states containing up to $N_{\max}$ HO excitations above the lowest possible configuration:

$$|\Psi_A^{J^\pi T}\rangle = \sum_{N=0}^{N_{\max}} \sum_i c_{Ni} |ANiJ^\pi T\rangle. \tag{1}$$

Here, N denotes the total number of HO excitations of all nucleons above the minimum configuration, $J^\pi T$ are the total angular momentum, parity and isospin, and i additional quantum numbers. The sum over N is restricted by parity to either an even or odd sequence. The basis is further characterized by the frequency Ω of the HO well and may depend on either Jacobi relative or single-particle coordinates. In the former case, the wave function does not contain the center of mass (c.m.) motion, but antisymmetrization is complicated. In the latter case, antisymmetrization is trivially achieved using Slater determinants, but the c.m. degrees of freedom are included in the basis. The HO basis within the $N_{\max}$ truncation is the only possible one that allows an exact factorization of the c.m. motion for the eigenstates, even when working with single-particle coordinates and Slater determinants. Calculations performed with the two alternative coordinate choices are completely equivalent.

Square-integrable energy eigenstates expanded over the $N_{\max}\hbar\Omega$ basis, $|ANiJ^\pi T\rangle$, are obtained by diagonalizing the intrinsic Hamiltonian, $\hat{H} = \hat{T}_{\text{int}} + \hat{V}$,

$$\hat{H} |A\lambda J^\pi T\rangle = E_\lambda |A\lambda J^\pi T\rangle, \tag{2}$$

where $\hat{T}_{\text{int}}$ is the internal kinetic energy operator and $\hat{V}$ is the NN or $NN+3N$ interaction. We note that with the HO basis sizes typically used ($N_{\max}\sim 10-14$), the $|A\lambda J^\pi T\rangle$ eigenstates lack correct asymptotic behavior for weakly-bound states and always have incorrect asymptotic behavior for resonances.

3.2 NCSM/RGM

In the NCSM/RGM [38, 41], the ansatz of Eq. (1) for the A-nucleon wave function is replaced by an expansion over antisymmetrized products of binary-cluster channel states $|\Phi_{\nu r}^{J^\pi T}\rangle$ and wave functions of their relative motion

$$|\Psi_A^{J^\pi T}\rangle \;\; = \;\; \sum_\nu \int dr\, r^2 \frac{\gamma_\nu(r)}{r} \hat{\mathcal{A}}_\nu |\Phi_{\nu r}^{J^\pi T}\rangle\,. \tag{3}$$

The channel states $|\Phi_{\nu r}^{J^\pi T}\rangle$ contain $(A-a)$- and a-nucleon clusters (with $a<A$) of total angular momentum, parity, isospin and additional quantum number $I_1, \pi_1, T_1, \alpha_1$ and $I_2, \pi_2, T_2, \alpha_2$, respectively, and are characterized by the relative orbital angular

momentum ℓ and channel spin $\vec{s} = \vec{I}_1 + \vec{I}_2$:

$$|\Phi_{\nu r}^{J^{\pi}T}\rangle = \left[\left(|A-a\ \alpha_1 I_1^{\pi_1}T_1\rangle\ |a\ \alpha_2 I_2^{\pi_2}T_2\rangle\right)^{(sT)} Y_{\ell}(\hat{r}_{A-a,a})\right]^{(J^{\pi}T)} \frac{\delta(r-r_{A-a,a})}{rr_{A-a,a}}. \quad (4)$$

The channel index ν collects the quantum numbers $\{A-a\ \alpha_1 I_1^{\pi_1}T_1; a\ \alpha_2 I_2^{\pi_2}T_2; s\ell\}$. The intercluster relative vector $\vec{r}_{A-a,a}$ is the displacement between the clusters' centers of mass and is given in terms of the single-particle coordinates $\vec{r}_i$ by:

$$\vec{r}_{A-a,a} = r_{A-a,a}\ \hat{r}_{A-a,a} = \frac{1}{A-a}\sum_{i=1}^{A-a}\vec{r}_i - \frac{1}{a}\sum_{j=A-a+1}^{A}\vec{r}_j. \quad (5)$$

The cluster wave functions depend on translationally invariant internal coordinates and are antisymmetric under exchange of internal nucleons, while the intercluster antisymmetrizer $\hat{\mathcal{A}}_{\nu}$ takes care of the exchange of nucleons belonging to different clusters.

With appropriate boundary conditions imposed on the wave functions of the relative motion $\gamma_{\nu}(r)$, the expansion of Eq. (3) is suitable for describing bound states, resonances and scattering states between clusters. For bound states, expansions (1) and (3) are equivalent, although for well-bound systems where short-range A-body correlations play a dominant role, the convergence of the eigenenergy would typically be more efficient within the NCSM model space defined by Eq. (1).

The unknown relative-motion wave functions $\gamma_{\nu}(r)$ are determined by solving the many-body Schrödinger equation in the Hilbert space spanned by the basis states $\hat{\mathcal{A}}_{\nu} |\Phi_{\nu r}^{J^{\pi}T}\rangle$:

$$\sum_{\nu}\int dr\, r^2 \left[\mathcal{H}_{\nu'\nu}^{J^{\pi}T}(r',r) - E\,\mathcal{N}_{\nu'\nu}^{J^{\pi}T}(r',r)\right]\frac{\gamma_{\nu}(r)}{r} = 0, \quad (6)$$

where

$$\mathcal{H}_{\nu'\nu}^{J^{\pi}T}(r',r) = \left\langle\Phi_{\nu'r'}^{J^{\pi}T}\right|\hat{\mathcal{A}}_{\nu'}\hat{H}\hat{\mathcal{A}}_{\nu}\left|\Phi_{\nu r}^{J^{\pi}T}\right\rangle, \quad (7)$$

$$\mathcal{N}_{\nu'\nu}^{J^{\pi}T}(r',r) = \left\langle\Phi_{\nu'r'}^{J^{\pi}T}\right|\hat{\mathcal{A}}_{\nu'}\hat{\mathcal{A}}_{\nu}\left|\Phi_{\nu r}^{J^{\pi}T}\right\rangle, \quad (8)$$

are the Hamiltonian and norm kernels, respectively, and E is the total energy in the c.m. frame.

3.3 NCSMC

The NCSMC ansatz for the many-body wave function includes both A-body square-integrable and $(A-a, a)$ binary-cluster continuous basis states according to:

$$|\Psi_A^{J^{\pi}T}\rangle = \sum_{\lambda} c_{\lambda} |A\lambda J^{\pi}T\rangle + \sum_{\nu}\int dr\, r^2 \frac{\gamma_{\nu}(r)}{r}\hat{\mathcal{A}}_{\nu}|\Phi_{\nu r}^{J^{\pi}T}\rangle. \quad (9)$$

The resulting wave function (9) is capable of describing efficiently both bound and unbound states. Indeed, the NCSM sector of the basis (eigenstates $|A\lambda J^{\pi}T\rangle$) provides an effective description of the short- to medium-range A-body structure, while the NCSM/RGM cluster states make the theory able to handle the scattering physics of the system. In other words, with the expansion (9) one obtains the coupling of the NCSM with the continuum. Clearly, the NCSMC model space is overcomplete, but this is not a concern. We also note that, in principle, the expansion (9) can be further generalized to include a three-cluster component suitable for the description of, e. g., Borromean halo nuclei and reactions with final three-body states [42].

The discrete (c_λ) and continuous $(\gamma_\nu(r))$ unknowns of the NCSMC wave function are obtained as solutions of the coupled equations

$$\begin{pmatrix} H_{NCSM} & \bar{h} \\ \bar{h} & \overline{\mathcal{H}} \end{pmatrix} \begin{pmatrix} c \\ \chi \end{pmatrix} = E \begin{pmatrix} 1 & \bar{g} \\ \bar{g} & 1 \end{pmatrix} \begin{pmatrix} c \\ \chi \end{pmatrix}, \tag{10}$$

where $\chi_\nu(r)$ are the relative wave functions in the NCSM/RGM sector when working with the orthogonalized cluster channel states [41]. These are related to the original wave functions $\gamma_\nu(r)$ of Eq. (9) by the relationship given in Eq. (20) of Ref. [40].

The NCSM sector of the Hamiltonian kernel is a diagonal matrix of the NCSM energy eigenvalues E_λ (2),

$$(H_{NCSM})_{\lambda\lambda'} = \langle A\lambda J^\pi T | \hat{H} | A\lambda' J^\pi T \rangle = E_\lambda \delta_{\lambda\lambda'} , \tag{11}$$

while $\overline{\mathcal{H}}$ is the orthogonalized NCSM/RGM kernel of Eq. (17) in Ref. [40]. Because of the orthogonalization procedure, both diagonal blocks in the NCSMC norm kernel are identities in their respective spaces. The coupling between square-integrable and binary-cluster sectors of the model space is described by the cluster form factor

$$\bar{g}_{\lambda\nu}(r) = \sum_{\nu'} \int dr' \, r'^2 \langle A\lambda J^\pi T | \hat{\mathcal{A}}_{\nu'} \Phi_{\nu'r'}^{J^\pi T} \rangle \, \mathcal{N}_{\nu'\nu}^{-\frac{1}{2}}(r', r) \tag{12}$$

in the norm kernel, and by the coupling form factor

$$\bar{h}_{\lambda\nu}(r) = \sum_{\nu'} \int dr' \, r'^2 \langle A\lambda J^\pi T | \hat{H} \hat{\mathcal{A}}_{\nu'} | \Phi_{\nu'r'}^{J^\pi T} \rangle \, \mathcal{N}_{\nu'\nu}^{-\frac{1}{2}}(r', r). \tag{13}$$

in the Hamiltonian kernel.

4   NCSM/RGM and NCSMC applications

4.1 ^{7}He resonances

The first demonstration of the power of the NCSMC approach was shown in an investigation of ^{7}He resonances [39,40]. The ^{7}He nucleus is a particle-unstable system with a $J^\pi T = 3/2^-$ $3/2$ ground state lying at 0.430(3) MeV [43,44] above the ^{6}He+n threshold and an excited $5/2^-$ resonance centered at 3.35 MeV, which mainly decays to $\alpha+3n$ (as discovered in the pioneering work of Ref. [45]). While there is a general consensus on the $5/2^-$ state, discussions are still open for the other excited states. In particular, the existence of a low-lying ($E_R \sim 1$ MeV) narrow ($\Gamma \leq 1$ MeV) $1/2^-$ state has been advocated by many experiments [46–50] while it was not confirmed in several others [51–56]. The presence of a low-lying $1/2^-$ state has been excluded by a study on the isobaric analog states of ^{7}He in ^{7}Li [57]. According to this work, a broad $1/2^-$ resonance at $\sim$3.5 MeV with a width $\Gamma \sim 10$ MeV fits the data the best. Neutron pick-up and proton-removal reactions [53,54] suggest instead a $1/2^-$ resonance at about 3 MeV with a width $\Gamma \approx 2$ MeV.

From a theoretical point of view, ^{7}He is an ideal system to showcase achievements made possible by a unified *ab initio* approach to nuclear bound and continuum states such as the NCSMC. Since ^{7}He is unbound, it cannot be reasonably described within the NCSM. One could calculate its properties using the NCSM/RGM within an ^{6}He+n binary-cluster expansion. However, the ^{6}He nucleus is weakly bound and all its excited states are unbound. Consequently, a limitation to just a few lowest ^{6}He eigenstates in the NCSM/RGM expansion would be questionable especially because, except for the lowest 2^+ state, all other ^{6}He excited states are either broad resonances or simply states in the continuum. With the NCSMC these challenges are overcome.

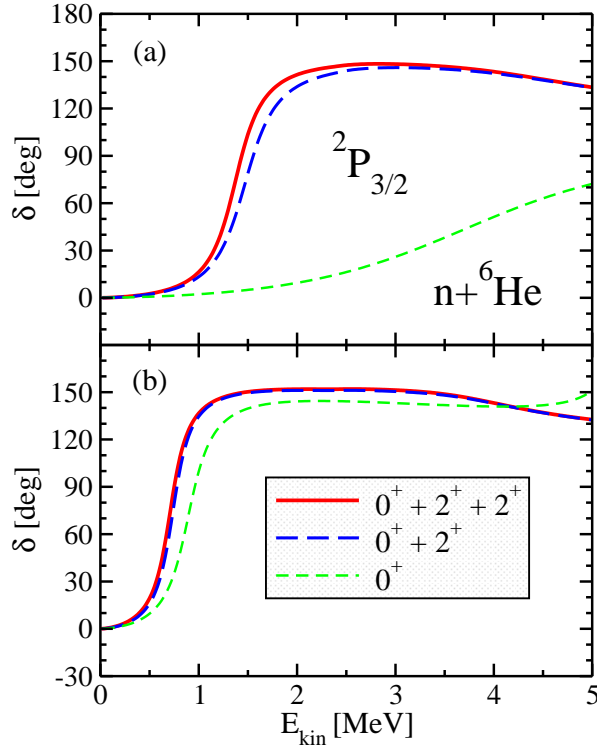Figure 1: Dependence of the NCSM/RGM (a) and NCSMC (b) ^{6}He+n phase shifts of the ^{7}He $3/2^-$ ground state on the number of ^{6}He states included in the binary-cluster basis. The short-dashed green curve, the dashed blue curve and the solid red curve correspond to calculations with ^{6}He 0^+ ground state only, $0^+, 2^+$ states and $0^+, 2^+, 2^+$ states, respectively. The similarity-renormalization-group (SRG) [58–61] N^{3}LO [62,63] NN potential with $\Lambda = 2.02$ fm^{-1}, the N_{max}=12 basis size and the HO frequency of $\hbar\Omega$=16 MeV were used.

This is seen by studying the dependence of the $3/2^-$ ground state (g.s.) phase shifts on the number of ^{6}He eigenstates included in the NCSM/RGM [panel (a)] and NCSMC [panel (b)] calculations, shown in Fig. 1. Here, the channels are denoted using the standard notation $^{2s+1}\ell_J$, e. g., $^2P_{3/2}$ for the g.s. resonance, with the quantum numbers s, ℓ and J defined as in Section 3.2, Eq. (4). We observe that the NCSM/RGM calculation with the ^{6}He target restricted to its ground state does not produce a ^{7}He $3/2^-$ resonance (the phase shift does not reach 90 degrees and is less than 70 degrees up to 5 MeV). A $^2P_{3/2}$ resonance does appear once $n+^6$He(2_1^+) channel states are coupled to the basis, and the resonance position further moves to lower energy with the inclusion of the second 2^+ state of ^{6}He. On the contrary, the NCSMC calculation with only the ground state of ^{6}He already produces the $^2P_{3/2}$ resonance. In fact, this NCSMC model space is sufficient to obtain the ^{7}He $3/2^-$ g.s. resonance at about 1 MeV above threshold, which is lower than the NCSM/RGM prediction of 1.39 MeV when three ^{6}He states are included. Adding the first 2^+ state of ^{6}He generates a modest shift of the resonance to a still lower energy while the 2_2^+ state of ^{6}He has no significant influence [see Fig. 1, panel (b)]. We further observe that the difference of about 0.7 MeV between the NCSM/RGM and NCSMC results for the resonance position is due to additional correlations in the wave function brought about by the ^{7}He eigenstates that are coupled to the neutron-^{6}He binary-cluster states in the NCSMC. Indeed, such $A = 7$ eigenstates (in the present calculation four $3/2^-$ states, of which only the $3/2_1^-$ produces a substantial effect on the $^2P_{3/2}$ resonance) have the practical effect of compensating for higher excited states of the ^{6}He target
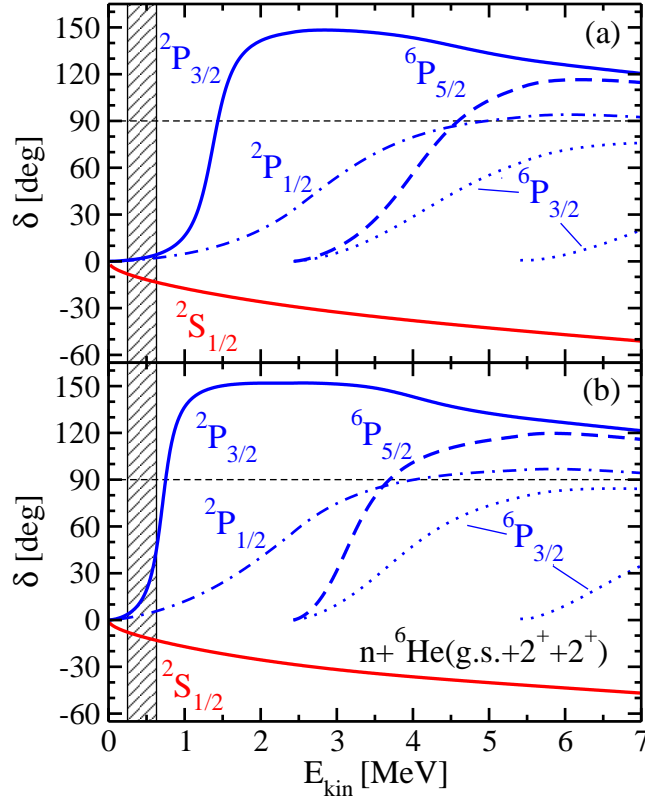
Figure 2: NCSM/RGM (a) and NCSMC (b) ^{6}He+n diagonal phase shifts (except $^6P_{3/2}$, which are eigenphase shifts) as a function of the kinetic energy in the center of mass. The dashed vertical area centered at 0.43 MeV indicates the experimental centroid and width of the ^{7}He ground state [43, 44]. In all calculations the lowest three ^{6}He states have been included in the binary-cluster basis.

omitted in the NCSM/RGM sector of the basis.

The NCSM/RGM and NCSMC phase shifts for the n+^{6}He five P-wave and the $^2S_{1/2}$ channels are shown in Fig. 2. All curves have been obtained including the three lowest ^{6}He states (i. e., the 0^+ ground state and the two lowest 2^+ excited states) within the $N_{\max} = 12$ HO basis. The model space of the NCSMC calculations [panel (b)] additionally includes ten ^{7}He NCSM eigenstates. The dashed vertical area centered at 0.43 MeV indicates the experimental centroid and width of the ^{7}He ground state [43, 44]. As expected from a variational calculation, the introduction of the additional square-integrable A-body basis states $|A\lambda J^\pi T\rangle$ [i. e., going from panel (a) to panel (b) of Fig. 2] lowers the centroid values of all ^{7}He resonances. In particular, the $3/2^-$ ground and $5/2^-$ excited states of ^{7}He are pushed toward the ^{6}He+n threshold, closer to their respective experimental positions. The resonance widths also shrink toward the observed data as we discuss below.

Computed widths Γ and resonance energies E_R are reported in Table 1, together with the available experimental data. From an experimental standpoint, the situation concerning the $1/2^-$ resonance is not clear as discussed in the beginning of this section and documented in Table 1. While the centroid energies determined in the experiments of Refs. [53, 54] and [57] are comparable, the widths are very different. Within the present determination of E_R and Γ, the NCSMC results are in fair agreement with the $1/2^-$ properties measured in the neutron pick-up and proton-removal reactions experiments of Refs. [53] and [54]. Our calculations definitely do not support the hypothesis of a low-lying ($E_R \sim 1$ MeV) narrow ($\Gamma \leq 1$ MeV) $1/2^-$ resonance [46–50].

Table 1: Experimental and theoretical values for the resonance centroids and widths in MeV for the $3/2^-$ ground state and the $5/2^-$ and $1/2^-$ excited states of ^{7}He. Calculations are carried out as described in Fig. 2 and in the text.

J^π	experiment			NCSMC		NCSM/RGM		NCSM
	E_R	Γ	Ref.	E_R	Γ	E_R	Γ	E_R
$3/2^-$	0.430(3)	0.182(5)	[44]	0.71	0.30	1.39	0.46	1.30
$5/2^-$	3.35(10)	1.99(17)	[64]	3.13	1.07	4.00	1.75	4.56
$1/2^-$	3.03(10)	2	[53]	2.39	2.89	2.66	3.02	3.26
	3.53	10	[57]					
	1.0(1)	0.75(8)	[47]					

4.2 Nucleon-^{4}He scattering with chiral $NN+3N$ interactions

The *ab initio* no-core shell model/resonating-group method has now been extended to include $3N$ interactions for the description of nucleon-nucleus collisions [65]. The extended framework was then applied to nucleon-^{4}He elastic scattering using similarity-renormalization-group evolved nucleon-nucleon plus three-nucleon potentials derived from chiral effective field theory. Up to six excited states of the ^{4}He target were included in the NCSM/RGM calculations. Significant effects from the inclusion of the chiral $3N$ force were found, e.g., it enhances the spin-orbit splitting between the $3/2^-$and $1/2^-$ resonances and leads to an improved agreement with the phase shifts obtained from an accurate R-matrix analysis of the five-nucleon experimental data. Calculated phase shifts compared to the R-matrix analysis of experimental data in the energy range up to the d-^{3}H threshold are shown in Fig. 3. The $^2P_{3/2}$ resonance position is overestimated. The probably reason is the omition of higher excited states of ^{4}He and of the other closed channels, e. g., d-^{3}H, in the calculations. The omitted states and channels can be effectively included by the NCSMC coupling to the ^{5}He eigenstates (obtained within the NCSM). Work in this direction is under way.

4.3 ^{6}He as a ^{4}He+n+n three-body cluster

The NCSM/RGM technique has also been generalized to the three-body cluster dynamics [42]. The solution of the three-cluster Schrödinger equation was obtained by means of hyperspherical harmonic expansions on a Lagrange mesh [67,68]. In Ref. [42], the first ^{4}He+n+n investigation of the g.s. of the ^{6}He nucleus was presented based on a NN potential that yields a high-precision fit of the NN phase shifts and *ab initio* four-body wave functions for the ^{4}He cluster obtained consistently from the same Hamiltonian. Within this approach, one gets the appropriate asymptotic behavior of the wave functions. This is demonstrated in Fig. 4 showing the ground-state wave function of ^{6}He. A two-peak shape distribution is found in the ground-state probability distribution. One peak corresponds to a "di-neutron" configuration in which the neutrons are close together (about 2 fm apart from each other) while the ^{4}He core is separated from their c.m. at a distance of about 3 fm. Whereas the second peak, corresponding to the "cigar" configuration, represents an almost linear structure in which the two neutrons are far from each other (about 5 fm apart) and the alpha particle lies almost in between them at ∼1 fm from their center of mass. Moreover, the present formalism combined with the appropriate scattering boundary conditions gives access to the *ab initio* study of resonant states of two-neutron halo nuclei (such as the excited states of ^{6}He) as well as to scattering problems involving channels with three fragments. Three-cluster NCSM/RGM ^{4}He+n+n scattering calculations with the aim to study the ^{6}He low-lying resonances are currently under way. Further, a generalization to include the NCSMC coupling is also under way.
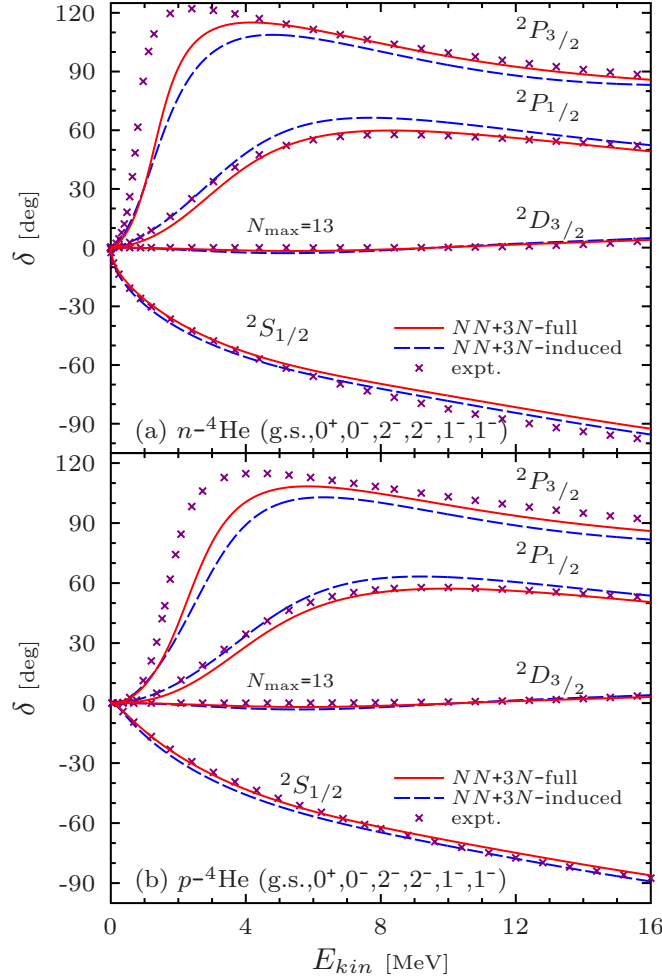
Figure 3: Comparison of the n-^{4}He (a) and p-^{4}He (b) phase-shifts ($^1S_{1/2}$, $^2P_{1/2}$, $^2P_{3/2}$ and $^2D_{3/2}$ waves) within the largest considered model space including the first six low-lying resonant states of the ^{4}He (g.s., 0^+0, 0^-0, 2^-0, 2^-1, 1^-1, 1^-0) at $N_{\max} = 13$ to the experimental phase-shifts (purple crosses) obtained from an R-matrix analysis [66]. Results for the $NN+3N$-full Hamiltonian are shown as red solid lines, those for the $NN + 3N$-induced Hamiltonian as blue dashed lines. For further details see Ref. [65]

4.4   Structure of ^{9}Be

The structure of ^{9}Be nucleus poses a challenge to *ab initio* approaches based on bound-state techniques such as the NCSM. The positive parity resonances are in general found too high compared to experiment and the splitting between the lowest $5/2^-$ and $1/2^-$ resonances tends to be overestimated when $3N$ effects are included [69]. A question is to which extend the continuum affects the ^{9}Be resonances and the above observations. NCSMC calculations with the chiral $NN+3N$ interactions are now under way to answer these questions. Here we discuss preliminary results obtained using only a two-nucleon SRG-evolved NN interaction. The ^{9}Be is studied as a system of ^{8}Be+n with g.s. and the 2^+ state of ^{8}Be included. The NCSMC coupling to the ^{9}Be NCSM eigenstates is taken into account. The n-^{8}Be P-wave phaseshifts are shown in Fig. 5. A good convergence with respect to the HO basis size is found. The ^{9}Be separation energy is overestimated by 1 MeV with the used NN potential, which then
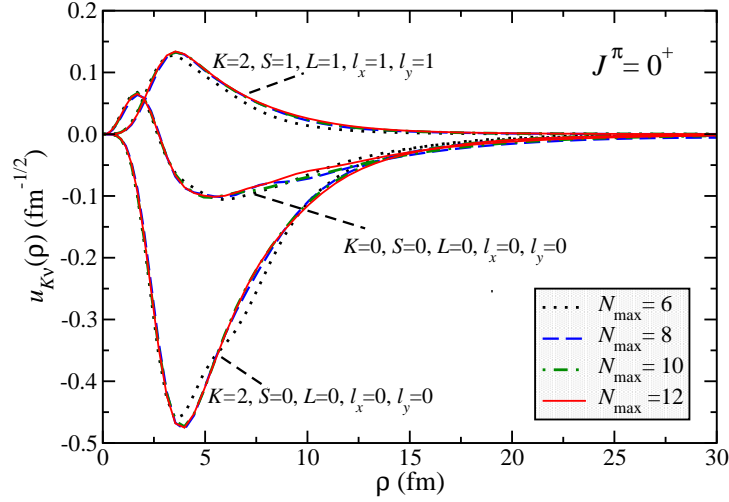
Figure 4: Three main components of the radial part of the ^{6}He g.s. wave functions as a dependence on the hyper-radius ρ for $N_{\max} = 6$, 8, 10, and 12. Further details can be found in Ref. [42]

also results in a shift of the resonances to a lower energy compared to experiment and even in a $\sim$100 keV binding of the $5/2^-$ state. Still, some interesting conclusions can be drawn even from these calculations. The splitting between the $5/2^-$ and the $1/2^-$ resonance is reduced substantially when the continuum is included due to the shift of the $1/2^-$ P-wave resonance with the $5/2^-$ F-wave state position unaffected. The positive-parity resonances, especially the $1/2_1^+$ and the $3/2_1^+$ S-wave resonances, are dramatically lowered in energy when the continuum is taken into account.
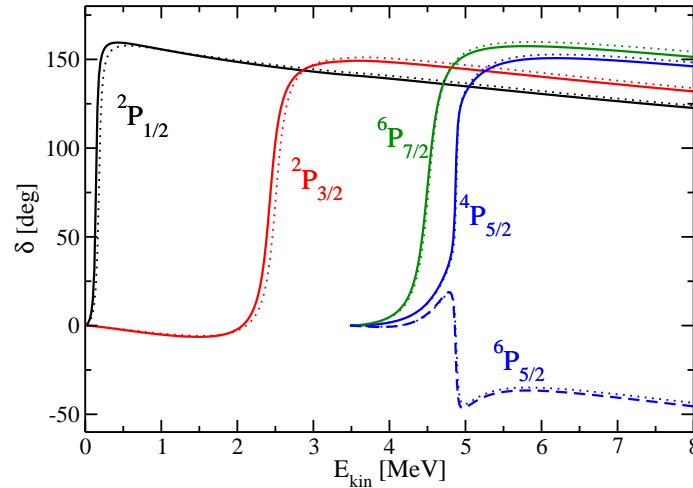

Figure 5: Preliminary results of n-^{8}Be phase shifts showing ^{9}Be P-wave resonances. The SRG-N^{3}LO NN potential with the evolution parameter $\Lambda = 2$ fm^{-1} was used. The full (dotted) lines correspond to the $N_{\max} = 10$ (8) model space, respectively. The HO frequency of 20 MeV was used.

5   Conclusions

Great progress has been made in the development of *ab initio* approaches to nuclear scattering, reactions and the description of weakly bound states. The accuracy of few-body methods improved and their ability to treat non-local and three-nucleon interactions has been extended. Nuclear reaction calculations with chiral forces are now possible. The four-nucleon scattering calculations are now feasible even above the breakup threshold. There are promising developments in methods applicable to systems of more than four nucleons. Continuum effects can now even be investigated in semi-magic nuclei beyond the p-shell.

We discussed in more details a new unified approach to nuclear bound and continuum states, the NCSMC, based on the coupling of a square-integrable basis (A-body NCSM eigenstates), suitable for the description of many-body correlations, and a continuous basis (NCSM/RGM cluster states) suitable for a description of long-range correlations, cluster correlations and scattering. This approach allows us to study weakly bound systems as well as narrow and broad resonances. The inclusion of $3N$ interactions in this formalism is under way. This opens new possibilities to perform realistic calculations for p- and light sd-shell nuclei starting from chiral $NN+3N$ interactions.

Acknowledgements

References

[1] B. S. Pudliner, V. R. Pandharipande, J. Carlson, S. C. Pieper and R. B. Wiringa, Phys. Rev. C **56**, 1720 (1997); R. B. Wiringa, S. C. Pieper, J. Carlson and V. R. Pandharipande, *ibid.* **62**, 014001 (2000); S. C. Pieper and R. B. Wiringa, Ann. Rev. Nucl. Part. Sci. **51**, 53 (2001); S. C. Pieper, K. Varga and R. B. Wiringa, Phys. Rev. C **66**, 044310 (2002).

[2] P. Navrátil, V. G. Gueorguiev, J. P. Vary, W. E. Ormand and A. Nogga, Phys. Rev. Lett. **99**, 042501 (2007).

[3] G. Hagen, T. Papenbrock, D. J. Dean and M. Hjorth-Jensen, Phys. Rev. Lett. **101**, 092502 (2008).

[4] G. Hagen, M. Hjorth-Jensen, G. R. Jansen, R. Machleidt and T. Papenbrock, Phys. Rev. Lett. **108**, 242501 (2012).

[5] R. Roth, S. Binder, K. Vobig, A. Calci, J. Langhammer and P. Navrátil, Phys. Rev. Lett. **109**, 052501 (2012).

[6] E. Epelbaum, H. Krebs, D. Lee and U.-G. Meissner, Phys. Rev. Lett. **106**, 192501 (2011).

[7] K. Wildermuth and Y. C. Tang, *A unified theory of the nucleus*. Vieweg, Braunschweig, 1977.

[8] P. Navrátil, J. P. Vary and B. R. Barrett, Phys. Rev. Lett. **84**, 5728 (2000); Phys. Rev. C **62**, 054311 (2000).

[9] H. Witała, W. Glöckle, J. Golak, A. Nogga, H. Kamada,R. Skibiński and J. Kuroś-Żołnierczuk, Phys. Rev. C **63**, 024007 (2001).

[10] R. Lazauskas and J. Carbonell, Phys. Rev. C **70**, 044002 (2004).

[11] R. Lazauskas, Phys. Rev. C **79**, 054007 (2009).

[12] A. Deltuva and A. C. Fonseca, Phys. Rev. C **75**, 014005 (2007).

[13] A. Deltuva and A. C. Fonseca, Phys. Rev. Lett. **98**, 162502 (2007).

[14] L. E. Marcucci, A. Kievsky, L. Girlanda, S. Rosati and M. Viviani, Phys. Rev. C **80**, 034003 (2009).

[15] D. Gazit, S. Bacca, N. Barnea, W. Leidemann and G. Orlandini, Phys. Rev. Lett. **96**, 112301 (2006).

[16] S. Quaglioni and P. Navrátil, Phys. Lett. B **652**, 370 (2007).

[17] S. Bacca, N. Barnea, W. Leidemann and G. Orlandini, Phys. Rev. Lett. **102**, 162501 (2009).

[18] H. M. Hofmann and G. M. Hale, Phys. Rev. C **77**, 044002 (2008).

[19] K. M. Nollett, S. C. Pieper, R. B. Wiringa, J. Carlson and G. M. Hale, Phys. Rev. Lett. **99**, 022502 (2007).

[20] S. Quaglioni and P. Navrátil, Phys. Rev. Lett. **101**, 092501 (2008).

[21] S. Quaglioni and P. Navrátil, Phys. Rev. C **79**, 044606 (2009).

[22] M. Chernykh, H. Feldmeier, T. Neff, P. von Neumann-Cosel and A. Richter, Phys. Rev. Lett **98**, 032501 (2007).

[23] R. Lazauskas, J. Carbonell, A. C. Fonseca, M. Viviani, A. Kievsky and S. Rosati, Phys. Rev. C **71**, 034004 (2005).

[24] M. Viviani, L. Girlanda, A. Kievsky, L. E. Marcucci and S. Rosati, EPJ Web Conf. **3**, 05011 (2010).

[25] M. Viviani, A. Kievski, L. Girlanda and L. E. Marcucci, Few-Body Syst. **45**, 119 (2009).

[26] A. Deltuva and A. C. Fonseca, Phys. Rev. C **86**, 011001(R) (2012).

[27] I. Brida, S. C. Pieper and R. B. Wiringa, Phys. Rev. C **84**, 024319 (2011).

[28] K. M. Nollett and R. B. Wiringa, Phys. Rev. C **83**, 041001(R) (2011).

[29] T. Neff, Phys. Rev. Lett. **106**, 04502 (2011).

[30] A. Kievsky, M. Viviani, P. Barletta, C. Romero-Redondo and E. Garrido, Phys. Rev. C **81**, 034002 (2010).

[31] Y. Suzuki, W. Horiuchi and K. Arai, Nucl. Phys. A **823**, 1 (2009).

[32] T. Luu, M. J. Savage, A. Schwenk and J. P. Vary, Phys. Rev. C **82**, 034003 (2010).

[33] J. Kirscher, H. G. Griesshammer, D. Shukla and H. M. Hofmann, Eur. Phys. J. A **44**, 239 (2010).

[34] G. Hagen, T. Papenbrock and M. Hjorth-Jensen, Phys. Rev. Lett. **104**, 182501 (2010).

[35] S. Bacca, N. Barnea, G. Hagen, G. Orlandini and T. Papenbrock, Phys. Rev. Lett. **111**, 122502 (2013).

[36] G. Hagen and N. Michel, Phys. Rev. C **86**, 021602 (2012).

[37] M. Pine, D. Lee and G. Rupak, arXiv:1309.2616 [nucl-th] (2013).

[38] S. Quaglioni and P. Navrátil, Phys. Rev. Lett. **101**, 092501 (2008).

[39] S. Baroni, P. Navrátil and S. Quaglioni, Phys. Rev. Lett. **110**, 022505 (2013).

[40] S. Baroni, P. Navratil and S. Quaglioni, Phys. Rev. C **87**, 034326 (2013), arXiv:1301.3450 [nucl-th] (2013).

[41] S. Quaglioni and P. Navrátil, Phys. Rev. C **79**, 044606 (2009).

[42] S. Quaglioni, C. Romero-Redondo and P. Navrátil, Phys. Rev. C **88**, 034320 (2013).

[43] R. H. Stokes and P. G. Young, Phys. Rev. Lett. **18**, 611 (1967); Phys. Rev. **178**, 2024 (1969).

[44] Z. X. Cao *et al.*, Phys. Lett. B **707**, 46 (2012).

[45] A. A. Korsheninnikov *et al.*, Phys. Rev. Lett. **82**, 3581 (1999).

[46] K. Markenroth *et al.*, Nucl. Phys. A **679**, 462 (2001).

[47] M. Meister *et al.*, Phys. Rev. Lett. **88**, 102501 (2002).

[48] F. Skaza *et al.*, Phys. Rev. C **73**, 044301 (2006).

[49] N. Ryezayeva *et al.*, Phys. Lett. B **639**, 623 (2006).

[50] V. Lapoux *et al.*, J. Phys. Conf. Ser. **49**, 161 (2006).

[51] H. G. Bohlen *et al.*, Phys. Rev. C **64**, 024312 (2001).

[52] G. V. Rogachev *et al.*, Phys. Rev. Lett. **92**, 232502 (2004).

[53] A. H. Wuosmaa *et al.*, Phys. Rev. C **72**, 061301 (2005).

[54] A. H. Wuosmaa *et al.*, Phys. Rev. C **78**, 041302 (2008).

[55] D. H. Denby *et al.*, Phys. Rev. C **78**, (2008) 044303.

[56] Yu. Aksyutina *et al.*, Phys. Lett. B **679**, 191 (2009).

[57] P. Boutachkov *et al.*, Phys. Rev. Lett. **95**, 132502 (2005).

[58] S. K. Bogner, R. J. Furnstahl and R. J. Perry, Phys. Rev. C **75**, 061001 (2007).

[59] R. Roth, S. Reinhardt and H. Hergert, Phys. Rev. C **77**, 064003 (2008).

[60] R. Roth, T. Neff and H. Feldmeier, Progr. Part. Nucl. Phys. **65**, 50 (2010).

[61] S. K. Bogner, R. J. Furnstahl and A. Schwenk, Progr. Part. Nucl. Phys. **65**, 94 (2010).

[62] D. R. Entem and R. Machleidt, Phys. Rev. C **68**, 041001 (2003).

[63] R. Machleidt and D. R. Entem, Phys. Rept. **503**, 1 (2011).

[64] D. R. Tilley *et al.*, Nucl. Phys. A **708**, 3 (2002).

[65] G. Hupin, J. Langhammer, P. Navrátil, S. Quaglioni, A. Calci and R. Roth, arXiv:1308.2700 [nucl-th] (2013).

[66] G. M. Hale, *private communication.*

[67] P. Descouvemont, C. Daniel and D. Baye, Phys. Rev. C **67**, 044309 (2003).

[68] P. Descouvemont, E. Tursunov and D. Baye, Nucl. Phys. A **765**, 370 (2006).

[69] C. Forssén, P. Navrátil, W. E. Ormand and E. Caurier, Phys. Rev. C **71**, 044312 (2005).

[70] Information on Titan can be found at the URL http://www.nccs.gov.